JOURNAL OF GEOPHYSICAL RESEARCH, VOL. 101, NO. A3, PAGES 4813–4823, MARCH 1, 1996

Current sheets in the solar minimum corona

S. E. Gibson and F. Bagenal

Astrophysical, Planetary, and Atmospheric Sciences Department, University of Colorado, Boulder

B. C. Low

High Altitude Observatory, National Center for Atmospheric Research

Abstract.
We analytically combine stress-free current sheets with a coronal magnetostatic bulk current model. We begin by imposing a current sheet at the equator as an upper boundary condition on the modeled coronal field. We find that in order to reproduce the sharp gradients across the boundaries of helmet streamers, we also have to add current sheets along the interface between open and closed field lines. We find a description of coronal magnetic field and density in the presence of both bulk and sheet currents that matches both white light and photospheric magnetic flux observations.

Introduction

The large-scale structures of the corona are shaped by the presence of magnetic fields and the solar wind. Neither the coronal magnetic field nor the solar wind flow can be measured directly with useful spatial resolutions. Theoretical models are therefore essential interpretive tools for understanding observed density structures in terms of their interactions with the magnetic field and the wind flow. Within about three solar radii in heliocentric distance, the quiescent corona is in approximate static equilibrium. This is true for the plasma in the magnetically closed regions since there can be no significant flow across the magnetic fields under the typical coronal conditions of high electrical conductivity. It is also true for the plasma in the magnetically open regions along which the solar wind does flow out into interplanetary space. Although the wind has a supersonic terminal speed in the outer corona, its speed in the inner corona is basically subsonic and negligible.

In modeling the inner corona as an atmosphere in static equilibrium, it is important to allow for the presence of electric currents flowing across the coronal magnetic field. The Lorentz force associated with these currents gives rise to the nonspherical corona commonly observed in scattered white light. The model constructed by *Bogdan and Low* [1986] (B&L) allows for cross-field currents in a volumetric distribution described by a single parameter. This model is a simple mathematical extention of the potential model, with the versatility of allowing for fully three-dimensional variations. Recent studies have used this model to interpret the observed white-light corona in relation to magnetograph observations of the photospheric magnetic fields [*Bagenal and Gibson,* 1991; *Gibson and Bagenal,* 1995]. These studies show that the B&L model is able to account for the nonsphericity of the corona over the largest scales in terms of bulk currents in the corona. However, over the smaller spatial scales, the model is not adequate. For example, the sharp boundaries of coronal density enhancements cannot be modeled. This is not surprising because the model current distribution is highly simplified, based on only a single parameter.

In the present paper, we extend the B&L model to allow for the presence of concentrated electric currents, in addition to the bulk currents, in the corona. To deal with the simplest form of the problem, we treat the model in axisymmetry which is a reasonable approximation for the corona at activity minimum. As we shall see, the addition of sheet currents allows for a better fit of the model to observations. In particular, the sharp boundaries of density enhancements can be modeled. We begin by discussing the magnetostatic models to be combined and then show how the result can be applied to observations of white light and photospheric magnetic field to quantify the physical properties of the corona during solar minimum.

Models

In this section, we describe the magnetostatic models to be used in our observational interpretation. Coronal structures are magnetic in origin, and it follows that the success of a model depends on how well it is able to capture the basic form of the large-scale coronal magnetic field. We begin by laying down in general terms the physics underlying the magnetostatic models.

Physical Considerations

Many models of the solar wind and MHD models of the corona derive wind velocities that are small com-

Paper number 95JA03477.
0148-0227/96/95JA-03477$05.00

pared to thermal and Alfvénic velocities in the lower corona. Specifically, the sonic point, where the wind velocity equals the thermal velocity, has been predicted to be between 3 and 6 solar radii [*Barnes,* 1992]. *Pneumann and Kopp*'s [1971] MHD simulation of the solar minimum corona, which allowed a wind as well as bulk and sheet currents, found a sonic point at 5 R_s at the equator and 4 R_s at the poles. More recently, *Habbal et al.* [1994] used white-light data and a two-fluid wind model and found a sonic point of 3.16 R_s in a coronal hole. From these results, we suggest that the assumption that the solar wind is basically subsonic in the lower corona is a reasonable one, specifically in the region that we will be studying in this paper, below 2.7 R_s. If the wind is subsonic, it does not significantly alter the corona from a static configuration (for example, the log of the density of an isothermal static corona is only changed by approximately 10% at the sonic point by the addition of an isothermal Parker wind [*Parker,* 1958]). We therefore assume that the wind plays a small or insignificant role in force balance at all latitudes in the regime we will study, so that a magnetostatic description is appropriate. However, we are not claiming that wind velocities in the solar corona have been conclusively established, either observationally or theoretically, and we bear in mind that should our assumption prove invalid, major modifications would have to be made in our analysis.

Although the inner corona is approximately in static equilibrium, the solar wind plays an important role in defining this equilibrium state. It is the competition between two opposing effects which produces the partially open, global magnetic field in the corona: the dominance of the solar wind in the outer corona which opens up the field and the tendency for the bipolar fields in the inner corona to seek a closed configuration. When treating the inner corona as a static state, the opening up of the far field by the solar wind is introduced into the model implicitly. This can be done by extending the static corona to infinity but demanding that the magnetic field is everywhere open beyond a specified radial distance. This critical radial distance is a free parameter of the model, set typically at about 3 R_s. The open far fields are associated with current sheets separating open fluxes of opposite polarities. These current sheets are stress-free surfaces of magnetic tangential discontinuities. The static problem for the global magnetic field then requires solving for the field with these current-sheet surfaces treated as unknown free surfaces in force balance with the field and plasma.

This free-boundary problem is in general formidable but is a more satisfactory approach than the traditional source-surface model. In the latter, the static corona is confined to a finite domain from the base of the corona out to a spherical surface, the source surface, where the magnetic field is constrained artificially to be radial by bulk currents outside this domain [*Schatten et al.,* 1969]. In this case, the field beyond the source surface is not described but is taken to be in an open configuration and dominated by the solar wind. The shape of the source surface is usually taken to be spherical for mathematical convenience. The partially open global field created by the source surface is a proxy for the actual field structure. In other words, the influence of the sheet currents that separate opposite fluxes in the far field on the magnetic field in the inner corona is simulated by the boundary conditions at the source surface. In any kind of static or dynamic equilibrium, the field is not likely to admit strictly radial magnetic fields on a spherical surface. The field topology in the source-surface model is therefore unreliable in the vicinity of the source surface. Overall, the assumption of a source surface is at best a crude approximation.

Zhao and Hoeksema [1994] combined the B&L bulk current model with current sheets at helmet streamer interfaces using a technique developed by *Schatten* [1971]. The magnetic field is calculated in an inner region below some "cusp surface" using the B&L model and the photospheric field as the lower boundary condition. At the cusp surface, the radial component of the magnetic field is reversed wherever it is negative. This effectively repels neighboring field lines at helmet streamer interfaces, pushing them open. The magnetic field in the outer region is obtained by using this cusp surface as an inner boundary condition and numerically matching the three components of the magnetic field at the cusp surface. The original polarity of the field lines is then restored, ensuring that $\nabla \cdot \mathbf{B} = 0$. This technique does provide a magnetic field that includes bulk currents and sheet currents, but because of the contrived way the field has been constructed, the field in the inner region is unaffected by the presence of the current sheets in the outer region. (The issue is being addressed by *Zhao et al.* [1995] in current research.) Moreover, the addition of the current sheets is essentially a numerical technique: the magnetic field in the two regions is matched numerically at the cusp surface using a least squares fit.

For our purpose in this paper, we will develop an analytic and globally consistent description of the coronal magnetized plasma in the presence of both bulk and sheet currents. We will avoid a direct treatment of the formidable free-boundary problem of the current sheet by limiting our consideration to a geometrically simple system, namely, one describing an axisymmetric corona which is also symmetric about its equator. The magnetic field is predominantly dipolar with a polarity inversion line coincident with the equator. This is the basic configuration of the corona at activity minimum. Given its symmetries, there is only one far-field current sheet separating the two hemispheres of opposite fluxes. It lies in the equator, extending out from some critical radial distance below which a fraction of the magnetic flux is in closed configuration. A rich family of analytic solutions describing the partially open global magnetic field embedding such a current sheet may be exploited for our modeling purpose [*Low,* 1986]. These magnetic fields are potential except at the current sheets. Figure 1a shows an example where it can be seen that the equatorial current sheet has an inner radial edge at the

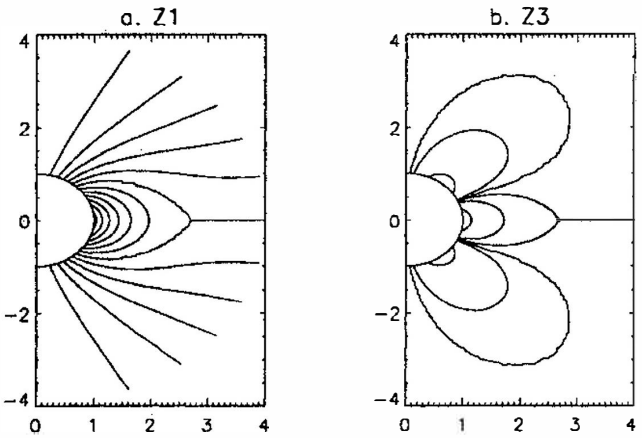

Figure 1. Contours of constant values of stream functions: (a) dipole Z_1 and (b) octopole Z_3.

Y-type magnetic neutral point. The separatrix lines of force passing through this neutral point separate the closed from the open lines.

Two other sources of electric current need to be introduced into the partially open potential field of *Low* [1986], if we are to account for the characteristic activity-minimum corona with its equatorial high-density helmet sandwiched between the extensive polar coronal holes. Let us identify the closed-field region in Figure 1a with the helmet and the open-field regions with the coronal hole; this is a widely accepted interpretation. Then, the observed sharp boundary of the helmet suggests that the separatrix lines coinciding with that boundary must contain concentrated electric currents. In the simplest approximation in the magnetostatic model, we may take the separatrix lines to be magnetic tangential discontinuities across which the total (magnetic and plasma) pressure is continuous. A discontinuous reduction of magnetic intensity across the separatrix lines going from the open into the closed-field regions will then be associated with a compensating discontinuous increase of plasma pressure and density. Thus the observed sharp boundary of the helmet can be modeled.

The remaining electric current mentioned above is of course the volumetric current density in addition to the discrete currents. The bulk current gives the atmosphere a continuous structure depending on its distribution. If the atmosphere contains only the current sheets in the far field and in the separatrix lines bounding the closed-field region, the field is potential everywhere except at these current sheets. The density will then only vary radially in a state of pure hydrostatic equilibrium, with discrete jumps across the separatrix lines. The continuous component of the coronal currents generates a departure from the radial stratification associated with the potential magnetic field.

We now turn to the details of the mathematical models.

Potential Fields With a Stress-Free Current Sheet

The classical potential problem $\nabla \times \mathbf{B} = 0$ for a magnetic field $\mathbf{B}$ can be extended to allow for the presence of stress-free current-sheet surfaces locally tangential to $\mathbf{B}$. Since $\nabla \cdot \mathbf{B} = 0$, the magnetic field in an axisymmetric system (i.e. no ϕ component) can be written in terms of a stream function A:

$$\mathbf{B}(r,\theta) = \frac{1}{r\sin\theta}\left(\frac{1}{r}\frac{\partial A}{\partial \theta}\hat{r} - \frac{\partial A}{\partial r}\hat{\theta}\right) \tag{1}$$

By transforming coordinate systems and superposing specialized potential fields, *Low* [1986] found a general set of solutions representing potential fields in the presence of a stress-free equatorial current sheet. The superposition involves potential fields which are functions of the inverted spheroidal coordinates u and v:

$$u^2 = -\frac{1}{2}\left(1 - \frac{b^2}{r^2}\right) + \frac{1}{2}\left[\left(1 - \frac{b^2}{r^2}\right)^2 + \frac{4b^2}{r^2}\cos^2\theta\right]^{\frac{1}{2}} \tag{2}$$

$$v^2 = -\frac{1}{2}\left(\frac{b^2}{r^2} - 1\right) + \frac{1}{2}\left[\left(\frac{b^2}{r^2} - 1\right)^2 + \frac{4b^2}{r^2}\cos^2\theta\right]^{\frac{1}{2}} \tag{3}$$

These potential fields are related to the classical spheroidal harmonics by the inversion transformation, which takes the disk singularity of these harmonics and spreads it out over an infinite current sheet of infinitesimal thickness lying at the equator with a circular hole of radius b centered at the origin. *Low* [1986] found stream functions of degree n:

$$Z_n(r,\theta) = S_n(r,\theta) + T_n(r,\theta) + \beta_n(r,\theta)U(r,\theta) \tag{4}$$

S_n represents the potential field solution to $\nabla \times \mathbf{B} = 0$ transformed to the $u - v$ coordinate system. T_n is added to eliminate the normal field component contributed by S_n at the current sheet. $\beta_n U$ is necessary to eliminate the remaining singularity of the combined field $S_n + T_n$ at the inner edge of the current sheet.

A generalized form for a potential field with an equatorial current sheet can then be written as a superposition of fields of different degree n, i.e. in terms of a combined potential field stream function

$$A_{\mathrm{pot}}(r,\theta) = \sum_n \gamma_n Z_n(r,\theta) \tag{5}$$

Here γ_n are constant coefficients. *Low* [1986] specifically calculated the dipole and octopole fields, Z_1 and Z_3 (see Appendix). Figure 1 shows the magnetic field lines traced by the contours of constant Z_1 and Z_3.

Bogdan and Low [1986] Bulk Current Model

Bogdan and Low [1986] found solutions in fully three-dimensional geometry to the magnetostatic force balance equations describing the corona, allowing for the presence of coronal bulk currents. To make an analytic three-dimensional solution tractable they assumed that the coronal currents were perpendicular to the Sun's gravitational field. They were then able to calculate a parameterized analytic description of the equilibrium magnetic field, density, and pressure.

In order to make contact with the *Low* [1986] current-sheet model, we recast the B&L solution in terms of the stream function A. (We will not actually specify A until the next section.) Meanwhile, since (1) gives the magnetic field in terms of A, the pressure is represented by

$$P(r,\theta) = P_o(r) + \frac{1}{8\pi}\left[\frac{1}{\eta(r)} - 1\right]\frac{1}{r^4\sin^2\theta}\left(\frac{\partial A}{\partial \theta}\right)^2 \quad (6)$$

and the density is

$$N_e(r,\theta) = \frac{R_s}{GM_\odot m_p}\left[\frac{\eta(r)-1}{8\pi}\frac{\partial}{\partial r}\left[\frac{1}{\sin^2\theta}\left(\frac{\partial A}{\partial r}\right)^2\right] - r^2\frac{\partial P}{\partial r}\right] \quad (7)$$

where

$$\eta(r) = \left(1 + \frac{a}{r}\right)^2 \quad (8)$$

and the spherically symmetric background pressure is

$$P_o(r) = \frac{c}{d+1}r^{-d-1} \quad (9)$$

The quantities r, a, and b are normalized to the solar radius R_s.

The parameter a can be interpreted as a scale length within which the majority of the currents are contained [*Low*, 1985]. Values of $a > 0$ correspond to a global geometric expansion of the magnetic field, and values of $a < 0$ correspond to compression relative to the special case $a = 0$ which is the case of a potential field. The spherically symmetric components of both pressure and density are parameterized as power laws, introducing the parameters c and d in (9). The expansion or contraction of the magnetic field that is mathematically generated by a nonzero a results in departures of the density distribution from spherical symmetry.

Combining Bulk and Current Sheet Models

The original formulation of the B&L model expresses the magnetic field B in terms of a bulk current function Φ, which contains the stretch or compression parameter a. If $a = 0$, the magnetic field is potential and can be written $\mathbf{B}_{\rm pot} = \nabla\Phi_{\rm pot}$, where $\Phi_{\rm pot}$ is the classical potential. The B&L bulk current function Φ and the potential function $\Phi_{\rm pot}$ are related by the transform $r \rightarrow r + a$. In the alternative formulation of the B&L model leading to (6) - (9), we represent the magnetic field $\mathbf{B}$ not in terms of Φ but in terms of a stream function A. If $a = 0$, the stream function A reduces to the stream function $A_{\rm pot}$ generating the potential field $\mathbf{B}_{\rm pot}$. Just as $\Phi_{\rm pot}$ and Φ are related by the transformation $r \rightarrow r + a$, so are $A_{\rm pot}$ and A. To introduce the B&L type of bulk currents into the current-sheet model is therefore a simple matter of calculating the stream functions $A_{\rm pot}$ for a potential field in the presence of a stress-free current sheet and then subjecting $A_{\rm pot}$ to the transformation $r \rightarrow r + a$. The equations for magnetic field, pressure, and density in the presence of both bulk currents and an equatorial current sheet then become

$$\mathbf{B}(r,\theta) = \frac{1}{r\sin\theta}\left(\frac{1}{r}\frac{\partial A_{\rm pot}(r')}{\partial\theta}\hat{r} - \frac{1}{1+a}\frac{\partial A_{\rm pot}(r')}{\partial r'}\hat{\theta}\right) \quad (10)$$

$$P(r,\theta) = P_o(r) + \frac{1}{8\pi}\left[\frac{1}{\eta(r)} - 1\right]\frac{1}{r^4\sin^2\theta}\left(\frac{\partial A_{pot}(r')}{\partial\theta}\right)^2 \quad (11)$$

and the density is

$$N_e(r,\theta) = \frac{R_s}{GM_\odot m_p}\frac{\eta(r)-1}{8\pi}\frac{\partial}{\partial r'}\left[\frac{1}{\sin^2\theta}\frac{1}{1+a}\left(\frac{1}{1+a}\frac{\partial A_{\rm pot}(r')}{\partial r'}\right)^2 - r^2\frac{\partial P}{\partial r}\right] \quad (12)$$

$$r' = \frac{r+a}{1+a} \quad (13)$$

Here r' has been normalized so that the bulk current radial magnetic field is identical to the potential radial magnetic field at the photosphere, i.e. where $r = 1$. $A_{\rm pot}$ is defined by (5), introducing the additional parameters γ_n.

Current Sheets Around the Helmet Streamer

Finally, we extend our analysis to include current sheets along the entire interface between open and closed-field lines. The stream function formulation of magnetic field and pressure allows us to add current sheets around this helmet streamer interface. The contour $A(r,\theta) = A_{\rm pot}(r',\theta) = 0$ traces the current sheet at the equator above the cusp of the helmet streamer. Below the cusp it traces the boundary between open and closed-field lines. We create a jump condition in the magnetic field across this interface by writing the stream function as

$$A(r,\theta) = A_{\rm pot}(r',\theta) = C_\alpha\sum_n \gamma_n Z_n(r',\theta) \quad (14)$$

where

$$\begin{aligned} C_\alpha &= \quad 1; \text{ closed field} \\ C_\alpha &= \quad C_{\rm open}(>1); \text{ open field} \end{aligned} \quad (15)$$

Since $\sum_n \gamma_n Z_n(r',\theta) = 0$ at the interface, the stream function is continuous, but its derivatives are not. Thus the magnetic field will have a jump in value across the interface between open and closed field lines, creating a current sheet.

In order to keep the current sheet stress free, the total pressure must be continuous across it, i.e., $\Delta\left(P + \frac{B^2}{8\pi}\right) = 0$. The jump in the derivatives of A causes a jump in both the magnetic field and the pressure due to bulk currents:

$$P_{\rm bulk} = \frac{1}{8\pi}\left[\frac{1}{\eta(r)} - 1\right]\frac{1}{r^4\sin^2\theta}\left(\frac{\partial A_{\rm pot}(r')}{\partial\theta}\right)^2 \quad (16)$$

We therefore add a jump $\Delta P(r)$ to the pressure in the open region to balance the total pressure across the interface.

At the interface

$$\begin{aligned} P_{\text{open}} &= P_o + P_{\text{bulk,open}} + \Delta P \\ &= P_o + C^2_{\text{open}} P_{\text{bulk,closed}} + \Delta P \end{aligned} \tag{17}$$

By defining

$$\Delta P = \left(1 - C^2_{\text{open}}\right)\left(\frac{B^2_{\text{closed}}}{8\pi} + P_{\text{bulk,closed}}\right) \tag{18}$$

it follows that

$$\begin{aligned} P_{\text{open}} &= P_o + P_{\text{bulk,closed}} + \\ &\quad \left(1 - C^2_{\text{open}}\right)\left(\frac{B^2_{\text{closed}}}{8\pi}\right) \\ &= P_{\text{closed}} + \left(1 - C^2_{\text{open}}\right)\left(\frac{B^2_{\text{closed}}}{8\pi}\right) \end{aligned} \tag{19}$$

resulting in

$$\frac{B^2_{\text{open}}}{8\pi} + P_{\text{open}} = \frac{B^2_{\text{closed}}}{8\pi} + P_{\text{closed}} \tag{20}$$

The preceding equations apply along the interface. The pressure jump ΔP is extrapolated into the open region as a change in spherically symmetric hydrostatic pressure. This step in the construction therefore introduces a jump in hydrostatic density ΔN in the open regime supported exactly by the pressure gradient force of ΔP. For each radius r along the interface the corresponding $\Delta P(r)$ is subtracted from all P_{open} at that height, since $(1 - C^2_{\text{open}})$ is negative for $C_{\text{open}} > 1$. The pressure at the interface will be less in the open region than the closed region, amd the net density will also decrease in the open region.

Application to Observations

Figure 2 shows observations of scattered white light in the corona for a day typical of solar minimum. Note that the corona is basically symmetric about the axis of rotation and the equator, allowing us to describe it in terms of the axisymmetric current-sheet model and eliminating the need for any odd n stream functions. This symmetry, combined with the quick dropoff with heliocentric radial distance of higher n stream functions, suggests that we can model the solar minimum struc-

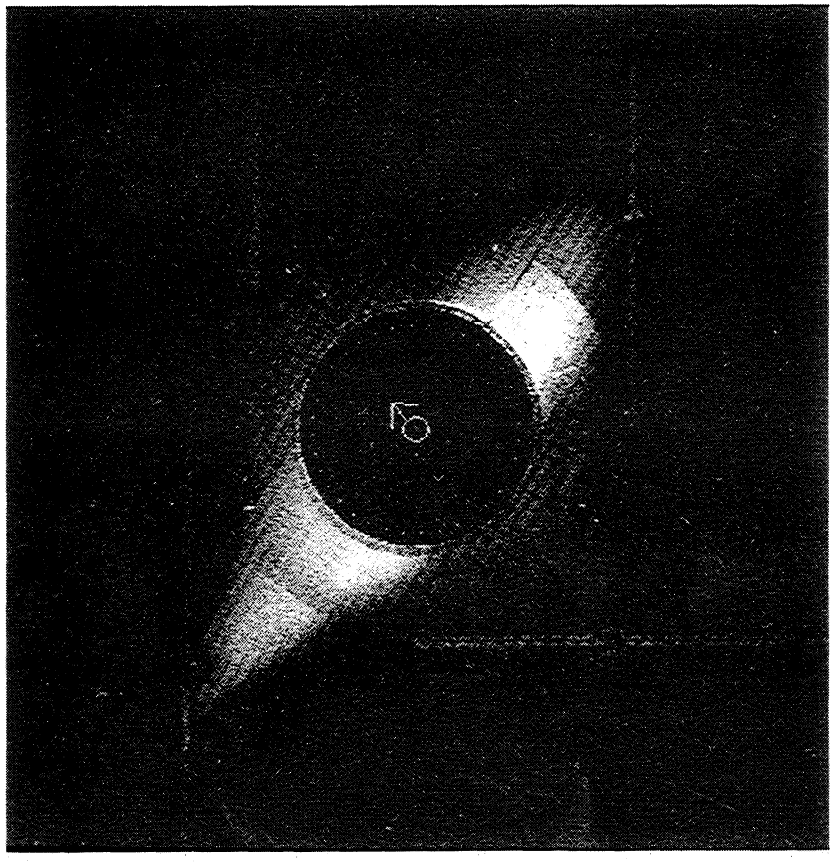

Figure 2. Observations of scattered light in the K-Corona for March 31,1986. the ground-based High Altitude Observatory Mark III K-Coronameter observes between 1.15 and 2.4 R_s, and the space-based Solar Maximum Mission Coronagraph/Polarimeter scans from 1.5 to 4.0 R_s. the data sets are patched together at r = 1.5 R_s. The one horizontal and three vertical streaks are due to instrumental artifacts.

ture using only the dipole and octopole stream functions presented in the Appendix. We shall see that just these two terms of the expansion in (14) are able to reproduce the general form of the observed corona.

Effect of Equatorial Current Sheet

Before we fit the full bulk current/current-sheet model developed above to observations, we first examine how the upper boundary condition of an equatorial current sheet relates to the coronal magnetic field and density. *Gibson and Bagenal* [1995] found a best fit to coronal white light and photospheric field observations, using the B&L bulk current model. In that work they used a source surface as the upper boundary condition on the magnetic field. The density, temperature, and magnetic field lines predicted by *Gibson and Bagenal* [1995] (Figure 3a - 3c) are compared to density, temperature, and magnetic field lines calculated with a current sheet at the equator but no jump condition around the helmet streamer as yet (Figure 3d - 3f). The B&L model pa-

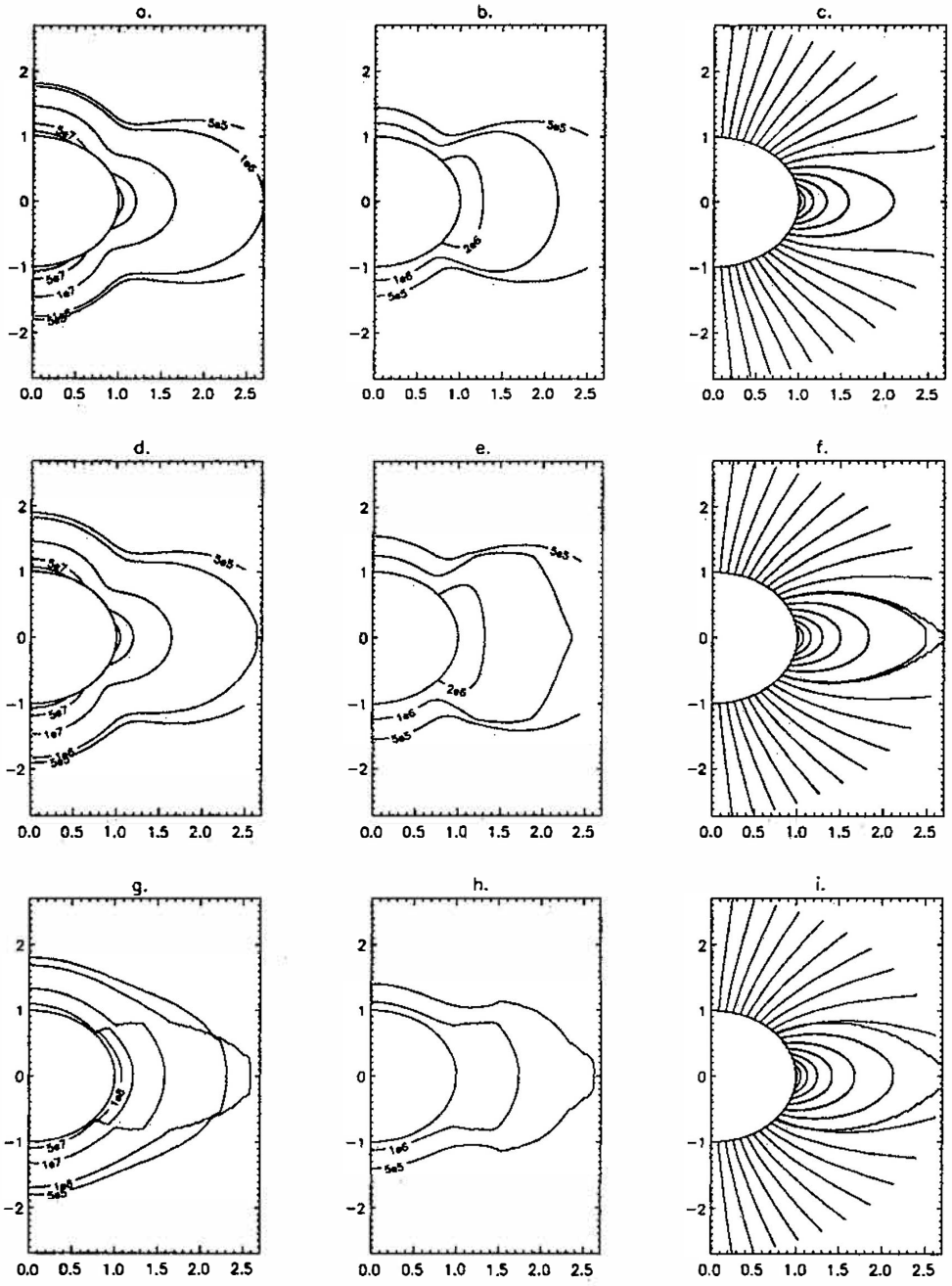

Figure 3. (a) Density, (b) temperature, and (c) magnetic field lines for the *Bogdan and Low*, [1986] model with source surface [*Gibson and Bagenal*, 1995]; (d) density, (e) temperature, and (f) magnetic field lines for the B&L bulk current model adapted to include a current sheet at the equator; and (g) density, (h) temperature, and (i) magnetic field lines for the best fit to the B&L bulk current model adapted to include current sheets along the interface between open and closed lines at the equator.

Table 1. Parameters Used in the Bulk Current/Current-Sheet Fit to White Light Data (Case 1) and the *Bogdan and Low*, [1986] Model Fit to White Light Data [*Gibson and Bagenal*, 1995] (Case 2).

Case	a	b	c	d	γ_1	γ_3	C_{open}
1	0.067	2.78	0.57	6.13	-2.4	1.2	1.27
2	0.5	2.7	0.59	5.25	-2.4	1.2	1.00

The parameters γ_1 and γ_3 exactly correspond to the parameters g_1^0 and g_3^0 used by *Gibson and Bagenal* [1995]. Parameters a, b, c, and d are normalized to R_s, γ_1 and γ_3 are in units of Gauss, and Copen is dimensionless.

rameters a, c, and d and the dipole and octopole magnetic field coefficients are identical for the two cases (the best fit of *Gibson and Bagenal* [1995] also had a small $n = 5$ component to the field, but it did not have a big effect on the large-scale structure, and we are ignoring it for this study). The only real difference between the two cases is that the *Gibson and Bagenal* [1995] case has a source surface at $r = 2.7\ R_s$ instead of an equatorial current sheet originating at $r = 2.7\ R_s$. The density and temperature are not greatly affected by the change in the upper boundary condition. (It should be borne in mind that the temperature has been calculated by taking the ratio of pressure to density and that no explicit energy equations have been solved.) The magnetic field, on the other hand, changes significantly. The magnetic field has a topology more closely resembling that produced by MHD numerical simulations of the coronal field, with a current sheet at the equator opening the far magnetic field and bending the field lines equatorwards [*Pneumann and Kopp*, 1971; *Linker et al.*, 1990; *Steinolfson et al.*, 1982].

Bulk Current/Current-Sheet Fit to Observations

We next examine how the sheet currents surrounding the helmet streamer and at the equator combine with the bulk currents to affect the coronal density and magnetic field. We use the magnetic field parameters from the *Gibson and Bagenal* [1995] fit to observations of scattered white light and photospheric magnetic flux and set the height of the equatorial current sheet to be $b = 2.78\ R_s$ (chosen as a best guess of the height of the cusp of the helmet streamer observed in white light). We then allow the current parameters a and Copen and the background density parameters c and d to vary.

Inverting the data in the manner described by *Gibson and Bagenal* [1995], we find that a choice of $a = 0.067\ R_s$ and Copen $= 1.27$ reproduces white-light observations reasonably well. This value of $a = 0.067\ R_s$ is significantly less than the value of $a = 0.5\ R_s$ found by *Gibson and Bagenal* [1995]. (See Table 1 for a complete listing of the parameters used in the two fits.) The jump in magnetic field and subsequently pressure across the current sheets surrounding the helmet streamer creates most of the density depletion at the poles, so that the bulk currents are only needed to adjust for variations from spherical symmetry in the open and closed regions. Figure 4a shows a contour plot of observations of scattered white light. Figure 4b shows the best fit to this data found by *Gibson and Bagenal* [1995], and Fig-

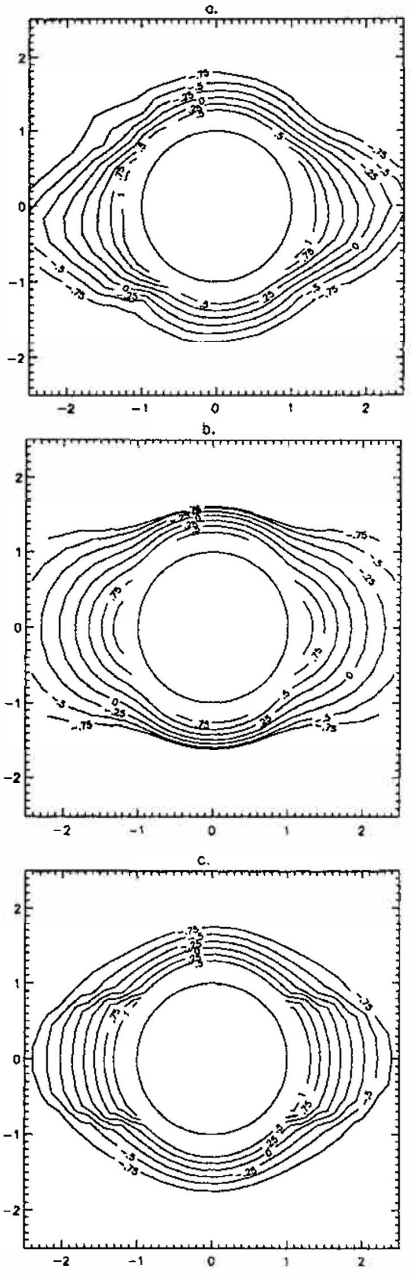

Figure 4. (a) Smoothed white-light data corresponding to Figure 2 for a day typical for solar minimum (March 31, 1986.) (b) Best fit to data using *Bogdan and Low*, [1986] bulk current model and a source surface [*Gibson and Bagenal*, 1995]. (c) Best fit to data using *Bogdan and Low*, [1986] bulk current model adapted to include current sheets along the interface between open and closed lines and at the equator.

ure 4c shows the fit to the bulk current/current-sheet model described above. Note that including currents around the helmet streamer introduces sharper gradients at midlatitude and also flattens out the profile at the poles. Overall, the fit to the data, in terms of the geometric form of the white-light corona, is markedly improved by the additional current sheets.

Gibson and Bagenal [1995] chose magnetic field coefficients that were compatible with observations of the photospheric field. Because the simple description of currents used in the B&L model might not be appropriate at the photosphere and because the white-light observations were on a much larger scale than the strong-field active regions observed at the photosphere, the authors did not attempt to match the photospheric field exactly. Instead, they constrained the magnetic field parameters such that the total modeled magnetic flux through each hemisphere of the photosphere was within the range of photospheric fluxes observed during the solar rotation containing the day corresponding to the white light data. In our bulk current/current sheet model, we have normalized the magnetic field such that the potential and bulk current solutions are identical at the photosphere (see (13)), so varying a will not affect the match to photospheric field observations. However, introducing $C_{\rm open}$ and thus the jump in magnetic field at the helmet streamer interface does affect the modeled field at $r \sim 1.0\ R_s$. Although we would not expect the discontinuity to extend all the way down to the photosphere, through regions where magnetic forces dominate and the plasma β is very small, our prediction of large-scale flux from the solar surface should still be in reasonable agreement with observations. With the value of $C_{\rm open} = 1.27$ determined from the fit to white-light data, the total magnetic flux through each hemisphere of the photosphere increases by about ten percent, still within the range of observed fluxes. In fact, the increase brings the predicted flux closer to the average flux observed [*Gibson and Bagenal,* 1995].

Figures 3g - 3i show the density, temperature, and magnetic field lines corresponding to our fit to data. A comparison of Figure 3g to Figure 3d shows that the inclusion of current sheets around the helmet streamer makes the density less rounded and with a sharper gradient across the open-closed field line interface. *Gibson and Bagenal* [1995] showed that the inclusion of both ground-based and space-based white-light data greatly reduced an earlier discrepancy between the B&L model predicted densities and densities predicted by other studies [see *Bagenal and Gibson*, 1991]. However, there remained a problem with the densities predicted by the B&L model at the poles for heights greater than about 1.7 R_s. Specifically, the densities dropped off too sharply at these heights. This was a problem inherent to the model. Figure 5 shows that by adjusting the B&L model to include current sheets around the helmet streamer and at the equator, we have created a model which allows a more gradual falloff in density at the

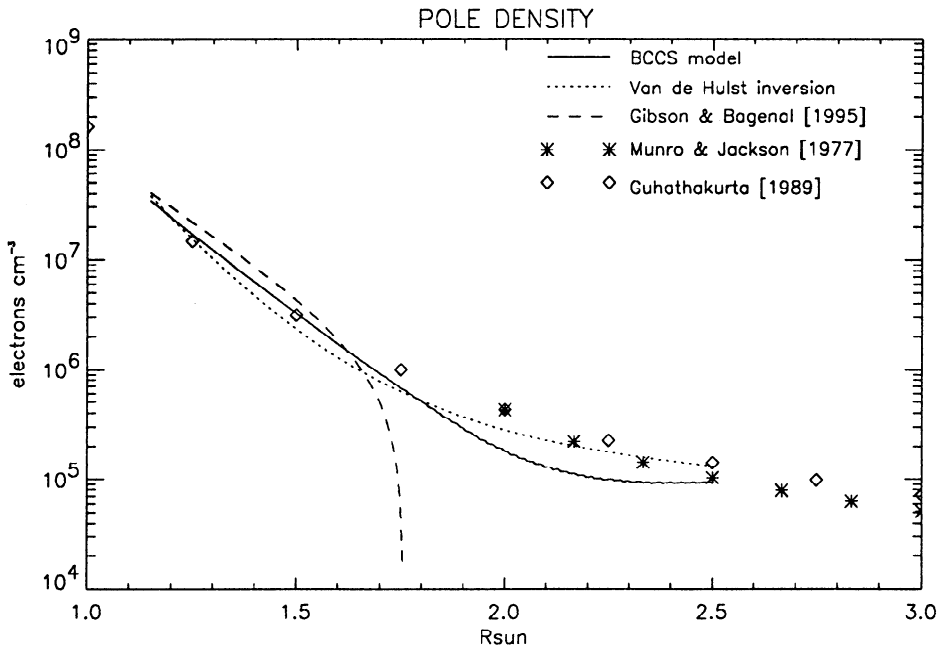

Figure 5. Comparison of magnetostatically modeled density predictions in the polar hole to those calculated via Van de Hulst inversion of the white-light data [Van de Hulst, 1950].(See also *Gibson and Bagenal* [1995] for a description of the Van de Hulst inversion technique.) The solid line in the density profile corresponding to the fit to white-light data using the bulk current/current-sheet (BCCS) model developed in this paper, and the dashed line is the fit to the B&L model described by *Gibson and Bagenal* [1995]. the dotted line is a Van de Hulst inversion of the same white-light data used in the magnetostatic models, and the asterisks and diamonds are densities predicted from Van de Hulst inversions of other white-light coronal polar hole data.

poles. We are therefore able to fit the white-light data better at the poles (see Figure 4), resulting in a density distribution that is meaningful at greater heights.

When we examine Figure 3, we find that including first an equatorial current sheet and then currents between open and closed magnetic field lines improves the correlation between the closed-field region and both the density and temperature enhancements at the helmet streamer. This has implications for the self-consistency of the magnetostatic models. Figure 6 shows the magnetic field extending out to 6 R_s predicted by the B&L bulk current model and by our new model which incorporates both bulk and sheet currents. In order to test the magnetostatic assumption, we have evolved a one-dimensional Parker wind [*Parker*, 1958] along the open field lines and marked the location of the sonic points on each open-field line with asterisks. In general, this sonic surface is well above the region that we have modeled (below 2.7 R_s), but for the B&L bulk current model the innermost open field lines have a wind that has accelerated to velocities comparable to the thermal velocity by 2.5 R_s. This is a direct result of the smaller closed-field region, which necessitates that the hot, dense, material of the helmet streamer overlies some open-field lines and accelerates the wind along these field lines to speeds inconsistent with the magnetostatic assumption. The bulk current/current-sheet model, on the other hand, is consistent with the magnetostatic assumption since none of the open-field lines lie beneath the helmet streamer. Indeed, the overlap of the helmet streamer and the closed-field lines is hardwired into the model through the jump conditions in magnetic field and pressure. We must emphasize here that such an evolution of a solar wind along the open-field lines is not meant as a rigorous solar wind solution but merely as a test of the self-consistency of the predicted field with model assumptions.

A final comment is that even with current sheets around the entire helmet streamer, we do not model the pointy nature of the tip of the closed-field region, or cusp (see Figure 4). This is because we have modeled the cusp as a *Y*-type triple point. In a *Y*-type point, the density jump must vanish with the field jump at that neutral point, so the density enhancement of the helmet is washed out in this vicinity. In order to model the point at the tip of the helmet streamer, we would need a magnetic field configuration with a true cusp point, i.e., where the discontinuity in the magnetic field remains finite, so that a higher helmet density is confined all the way to the cusp point [*Sturrock and Smith*, 1968]. Such a magnetic feature lies outside the capability of our models, however.

Conclusions

By combining the models of *Bogdan and Low* [1986] and *Low* [1986], we have established an analytic and self-consistent technique to model the large-scale solar

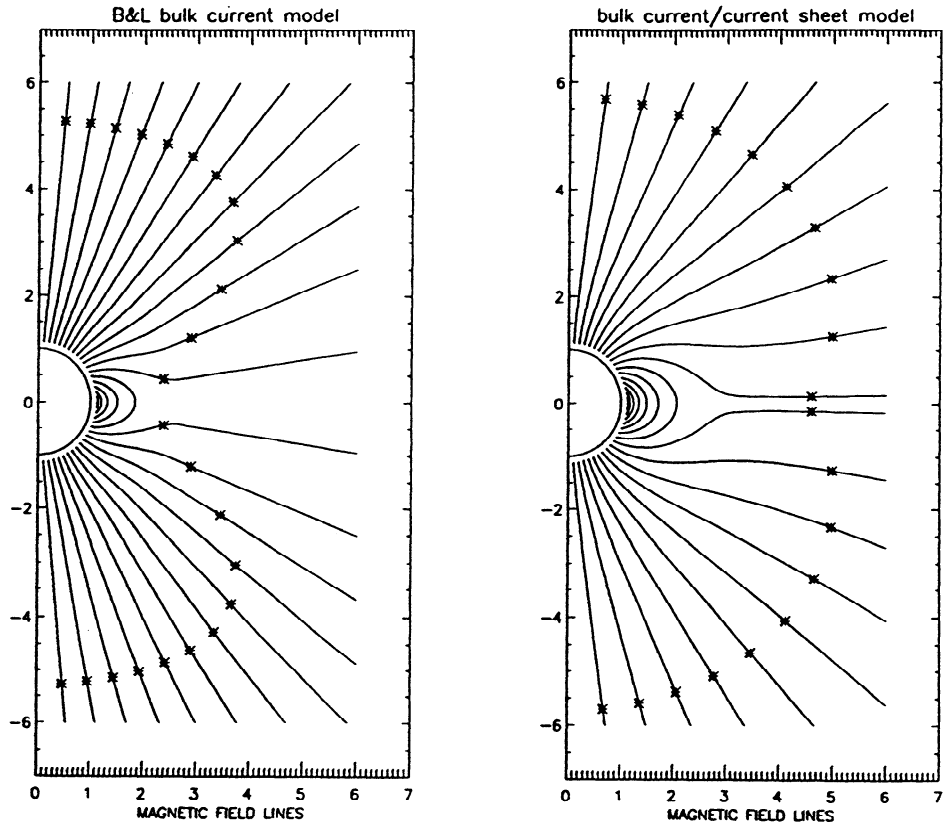

Figure 6. Magnetic field lines corresponding to Figure 3c and 3h, extended out to six solar radii. The asterisks show the sonic surface.

minimum coronal magnetic field and density in static equilibrium with bulk and sheet currents. In reality, the white-light corona is of course rich with other structures not mentioned above, even at activity minimum. For example, the helmet usually reveals concentric looplike structures in its bright region and a low-density cavity containing a quiescent prominence at its base [*Saito and Tandberg-Hanssen,* 1973]. We have made no attempt to model these and other structures. Our limited goal has been to improve on the results of *Gibson and Bagenal* [1995] by bringing the *Bogdan and Low* [1986] model a step closer to the observed minimum-activity corona by including discrete current sheets. From Ampere's law, the coronal magnetic field is due to the superposition of magnetic fields due to electric currents flowing below the corona and in the corona. The currents below the corona give a potential field in the corona. This potential field is modified by the currents in the corona. With our interest centered only on the large-scale corona, we have introduced the equatorial current sheet which creates the open part of the magnetic flux; an effect ultimately due to the solar wind. We have also introduced the current sheet expected at the boundary of the helmet structure. Finally, we have included the simple one-parameter volumetric currents of the *Bogdan and Low* [1986] model. By including both bulk and sheet currents in this systematic manner, we have accounted for the electric currents which control the large-scale topology of the coronal magnetic field at activity minimum. The resulting magnetic field predicts a self-consistent coronal density distribution in static equilibrium. We have shown that this modeled density distribution matches white-light observations significantly better than the density distribution predicted by a less complete model. We have therefore made progress in relating the observed large-scale corona (at minimum) to its, unobserved, large-scale magnetic field.

Appendix: Dipole and Octopole Stream Functions

Low [1986] calculated the dipole and octopole stream functions Z_1 and Z_3. Note that the Z_n are not orthonormal: Z_3 contains some dipole stream function. This is necessary to cancel the stresses at the current sheet. Note also that our Z_1 and Z_3 differ from those presented in the paper by *Low* [1986] by normalizing factors of $\frac{2}{\pi b^2}$ and $\frac{-1}{45\pi b^4}$, respectively. These have been included so that the fields reduce to the standard potential dipole and octopole fields when $b \to \infty$. Finally, r, b, and radial derivatives are dimensionless and normalized to R_s throughout this paper.

$$Z_1 = \frac{2}{\pi b^2}\left(r(1-v^2)\left[(1+u^2)\tan^{-1}\frac{1}{u} - u\right]\right) - \frac{\sin^2\theta}{r} + \frac{2}{\pi b}U \tag{A1}$$

$$Z_3 = \left(\frac{-1}{45\pi b^4}\right)\left(\frac{3}{4}\right)\left[r(1-v^2)(5v^2-1)\left(-3(1+u^2)(5u^2+1)\tan^{-1}\frac{1}{u} + 15u^3 + 13u\right)\right] - \frac{1}{8}\frac{\sin^2\theta(5\cos^2\theta-1)}{r^3} - \frac{1}{10b^2}\frac{\sin^2\theta}{r} - \frac{12}{45\pi b^3}U \tag{A2}$$

$$U = \eta \quad \theta > \tfrac{\pi}{2}$$
$$U = -\eta \quad \theta < \tfrac{\pi}{2} \tag{A3}$$

The spheroidal coordinate η is related to the coordinate v by inversion with respect to a sphere of radius b centered at the origin (see (3)):

$$\eta^2 = -\frac{1}{2}\left(\frac{r^2}{b^2} - 1\right) + \frac{1}{2}\left[\left(\frac{r^2}{b^2} - 1\right)^2 + \frac{4r^2}{b^2}\cos^2\theta\right]^{\frac{1}{2}} \tag{A4}$$

Acknowledgments. The Editor thanks M. Guhathakurta and another referee for their assistance in evaluating this paper.

References

Bagenal, F., and S. E. Gibson, Modeling the large scale structure of the solar corona, *J. Geophys. Res.*, *96*, 17,663, 1991.

Barnes, A., Acceleration of the solar wind, *Rev. Geophys.*, *30*, 4 3, 1992.

Bogdan, T. J., and B. C. Low, The three-dimensional structure of magnetic atmospheres, II, Modeling the large-scale corona, *Astrophys. J.*, *306*, 271, 1986.

Gibson, S. E., and F. Bagenal, The large-scale magnetic field and density distribution in the solar minimum corona, *J. Geophys. Res.*, *100*, 19,865, 1995.

Guhathakurta, M., The large and small-scale density structure in the solar corona, thesis, Univ. of Denver, Lab. for Atmos. and Space Phys. cooperative thesis, Boulder, Colorado, 1989.

Habbal, S. R., R. Esser, M. Guhathakurta, and R. Fisher, Flow properties of the solar wind obtained from white-light data and a two-fluid model, in *Proceedings of the Third SOHO Workshop, Eur. Space Agency Spec. Publ., ESA SP-373*, 211, 1994.

Linker, J. A., G. Van Hoven, and D. D. Schnack, A three-dimensional simulation of a coronal streamer, *Geophys. Res. Lett.*, *17*, 2281, 1990.

Low, B. C., The three-dimensional structure of magnetic atmospheres, I, Theory, *Astrophys. J.*, *293*, 31, 1985.

Low, B. C., Models of partially open magnetospheres with and without magnetodisks, *Astrophys. J.*, *310*, 953, 1986.

Munro, R. H., and B. V. Jackson, Physical properties of a polar coronal hole from 2 to 5 R_s, *Astrophys. J.*, *213*, 874, 1977.

Parker, E. N., Dynamics of the interplanetary gas and magnetic field, *Astrophys. J.*, *128*, 664, 1958.

Pneumann, G. W., and R. A. Kopp, Gas-magnetic field interactions in the solar corona, *Sol. Phys.*, *18*, 258, 1971.

Saito, K., and E. Tandberg-Hanssen, The arch systems, cavities and prominences in the helmet streamer observed at the solar eclipse, November 12, 1966, *Sol. Phys.*, *31*, 105, 1973.

Schatten, K. H., Current sheet magnetic model for the solar corona, *Cosmic Electrodyn., 2*, 232, 1971.

Schatten, K. H., J. M. Wilcox, and N. Ness, A model of interplanetary and coronal magnetic fields, *Sol. Phys., 6*, 442, 1969.

Steinolfson, R. S., S. T. Suess, and S. T. Wu, The steady global corona, *Astrophys. J., 255*, 730, 1982.

Sturrock, P. and Smith, S., Magnetic-field structure associated with coronal streamers, *Sol. Phys., 5*, 87, 1968.

Van de Hulst, H. C., The electron density of the solar corona, *Bull. Astron. Inst. Neth., 11*, 135, 1950.

Zhao, X. P., and J. T. Hoeksema, A coronal magnetic field model with horizontal and sheet currents, *Sol. Phys., 151*, 91, 1994.

Zhao, X. P., J. T. Hoeksema, and P. H. Scherrer, Potential contribution of MDI to understanding large-scale structures in the corona, in *Fourth SOHO Proceedings, Eur. Space Agency Spec. Publ.*, ESA, SP-376, 201, 1995.

S. E. Gibson and F. Bagenal, Astrophysical, Planetary, and Atmospheric Sciences Department, University of Colorado, Campus Box 391, Boulder, CO 80309-0391. (e-mail: gibson@dosxx.colorado.edu)

B.C Low, High Altitude Observatory, National Center for Atmospheric Research, Boulder, CO.

(Received July 24, 1995; revised November 6, 1995; accepted November 10, 1995.)